

Ab initio Investigation of Adsorption Characteristics of Bisphosphonates on Hydroxyapatite (001) Surface

Mun-Hyok Ri^a, Yong-Man Jang^b, Chol-Jun Yu^{*a}, and Song-Un Kim^b

Received Xth XXXXXXXXXXXX 20XX, Accepted Xth XXXXXXXXXXXX 20XX

First published on the web Xth XXXXXXXXXXXX 200X

DOI: 10.1039/b000000x

The structures of some bisphosphonates (clodronate, etidronate, pamidronate, alendronate, risedronate, zoledronate, minodronate) were obtained and analyzed, and their adsorption energies onto hydroxyapatite (001) surface were compared to find out ranking order of binding affinity, which shows that the adsorption energy is the largest for pamidronate, followed by alendronate, zoledronate, clodronate, ibandronate, the lowest for minodronate and etidronate.

1 Introduction

Bisphosphonates (BPs) are now widely used for the treatment of metabolic bone diseases including osteoporosis, Paget's disease and bone metastases^{11,15,33,36,37}. In addition, BPs are also useful as novel ligands for well-defined radioactive metal complexes that can be used both for bone scanning imaging and for therapeutic applications⁴⁸. BPs have high affinity for calcium ions and therefore bind strongly to the principal bone mineral, hydroxyapatite (HAP), where they are internalized by bone-resorbing osteoclasts and inhibit their function^{16,19,23,24}.

BPs are metabolically stable analogues of inorganic pyrophosphate (PPi), a naturally occurring modulator of calcification. Stability is conferred by a carbon atom replacing the oxygen atom which connects two phosphonates. BPs of medical interest all have two phosphonate groups sharing a common carbon atom between them (Figure 1). BPs have chemical and

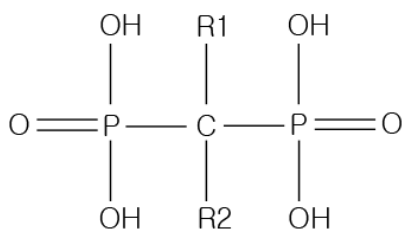


Fig. 1 General Structure of BPs

physical properties similar to pyrophosphate^{20,34} but, due to

^a Department of Computational Materials Design (CMD), Faculty of Materials Science, Kim Il Sung University, Ryongnam-Dong, Taesong-District, Pyongyang, Democratic People's Republic of Korea.

^b Department of Organic Chemistry, Faculty of Chemistry, Kim Il Sung University, Ryongnam-Dong, Taesong-District, Pyongyang, Democratic People's Republic of Korea.

their P-C-P backbone, they are considerably more resistant to heat and enzymatic hydrolysis. Both phosphonate groups are required, as modifications to one or both reduce the affinity¹⁴, as well as reduce biochemical potency^{13,45}. R1 substituents such as hydroxyl (OH) and amino (NH₂) can enhance chemical adsorption with their additional abilities to co-ordinate to calcium^{4,10}. Varying R2 substituent (Figure 2), the antiresorptive potency changes in several orders of magnitude¹⁴. Bisphosphonates with R2 chain containing a basic primary nitrogen atom in an alkyl chain (e.g., pamidronate, alendronate, and neridronate) are more potent antiresorptive than not containing nitrogen atom (e.g., clodronate and etidronate). More highly substitution of nitrogen atom in an alkyl chain (e.g., olpadronate and ibandronate) can display further increase in an antiresorptive potency⁴². The most potent antiresorptive bisphosphonates include those containing nitrogen atom within an heterocyclic ring (e.g., risedronate, zoledronate, and minodronate)^{27,28}. The overall pharmacological effects of BPs are mainly related to binding affinity for bone mineral (HAP) and inhibitory effects on osteoclasts¹¹.

Strong binding affinity of BPs on bone mineral can influence on some important biological properties of these drugs, including uptake and retention on bone, diffusion within bone, release from bone, and recycling back onto bone surface^{9,35}. The mineral binding affinity may also affect the appropriate dosing interval and the persistence of effect after discontinuation of medication^{7,17}. Therefore, binding affinity of BPs on bone mineral may play an important role on the pharmacological effects of these drugs.

There are some reports on experiments of measuring and comparing binding affinities of BPs on bone. By using a constant composition potentiostatic method, Nancollas et al studied the kinetic mineral binding affinities of bisphosphonates to identify zoledronate and alendronate as the higher affinity agents followed by ibandronate and risedronate¹⁸. Lawson

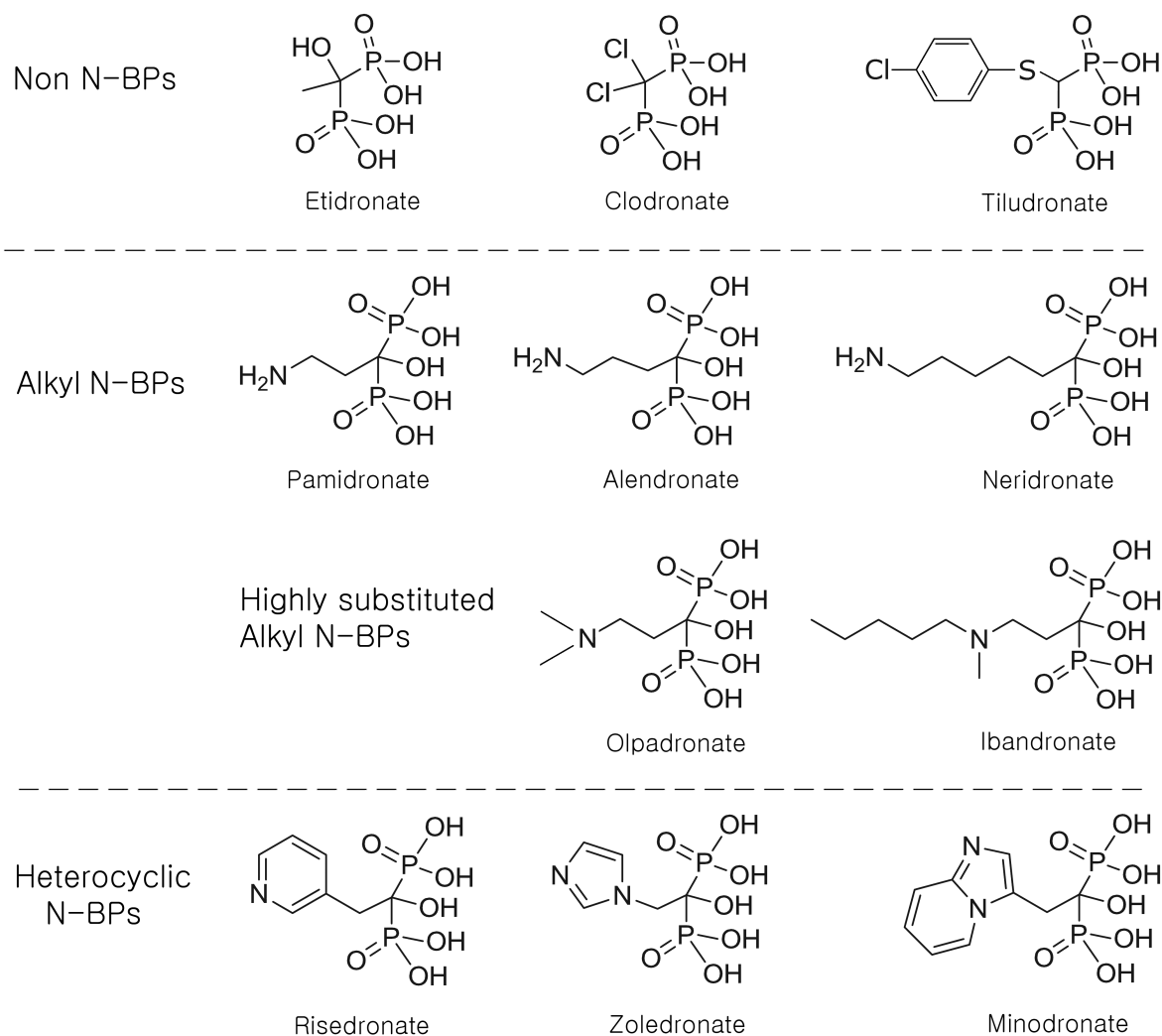


Fig. 2 Classification of BPs

and co-workers have developed FPLC (fast performance liquid chromatography) utilizing crystalline HAP, which showed that zoledronate had a longer retention time compared to risedronate, indicating a stronger binding affinity for HAP³⁰. Leu and co-workers studied bisphosphonate adsorption on human bone by competitive binding assays of radio-labeled bisphosphonates, which showed that most tested BPs, including etidronate, ibandronate, pamidronate, alendronate, risedronate, and zoledronate had comparable affinities, but tiludronate and especially clodronate displayed significantly weaker affinity for bone⁶. Jahnke et al, using NMR techniques, provided even more accurate comparison of thermodynamic binding affinities⁴⁶ that parallels the Leu rankings⁶. Mukherjee et al studied the thermodynamic properties of bis-

phosphonates binding to human bone in more detail using ³¹P NMR to obtain another set of affinity rankings^{40,41}, which showed that similar to the results of Nancollas et al¹⁸ risedronate has lower affinity, while zoledronate and alendronate have the highest affinity. In recent studies, mass spectrometry (MS) has been applied for specific identification and quantification of BPs, which has enabled the efficient separation and quantification of BPs with their binding affinities⁴⁹. The combination of FPLC with MS provides an accurate, precise, and robust method for quantitative analysis⁴⁹. Although there are some differences in ranking orders of BPs binding affinity among various adsorption assays, in general, amino-alkyl BPs including pamidronate, alendronate, and neridronate have the highest affinities, while clodronate has the lowest affinity, and

risedronate displays intermediate affinity (Table 1).

Table 1 Comparison of rank orders of HAP binding affinities of BPs among different adsorption assays

Ranking order	Exp ^a	Exp ^b	Exp ^c	Exp ^d	Exp ^e
1	ZOL	ALN	PAM	PAM	PAM
2	PAM	ZOL	ALN	ALN	ALN
3	ALN	PAM	ZOL	ETD	NER
4	IBN	RIS	RIS	NER	ETD
5	RIS	ETD	IBN	ZOL	ZOL
6	ETD	IBN		RIS	IBN
7	CLO	TIL		IBN	MIN
8		CLO		MIN	RIS
9				CLO	CLO

^a Constant composition kinetic studies of HAP crystal growth (Nancollas¹⁸)

^b Competitive binding assay of radio-labeled BPs (Leu⁶)

^c NMR-based competitive binding assay (Jahnke⁴⁶, Mukherjee^{40,41})

^d Fluorescence competitive binding assay (Duan⁴⁹)

^e HAP FPLC (Duan⁴⁹)

Structure-activity data in these studies show that small differences in BP structure lead to substantial changes in the three dimensional (3-D) shape and atomic orientation, resulting in significant changes in bone affinity.

Therefore, computational modeling and simulations are widely used to establish accurate and precise relationship between structure and bone affinity of BPs based on molecular and atomic level for development of further promising BPs^{8,12,31}. Modeling studies by Lawson et al³¹ indicated that N atoms in the BP side chains can coordinate with OH groups in HAP with bonding efficiencies related to their overall binding affinity. Comparative modeling of BPs by Ebetino et al¹² demonstrated that N atoms of BPs can form a N-H-O hydrogen bond to the labile OH and a bifurcated interaction at the P-O oxygen atoms of HAP (001) surface. Duarte et al⁸ performed molecular mechanics simulations for molecular structures of 18 novel hydroxyl- and amino-BPs to examine the interaction between BPs and HAP and to extract relating structural characteristics of BPs and their affinities for the mineral, which are in agreement with in vitro and in vivo studies for some of the studied BPs. These modeling and simulations are based on molecular mechanics with well-defined forcefields, that is not good for physico-chemical process such as adsorption of BPs on HAP surface accompanied with charge movement, in which density functional theory (DFT) provides reasonable results.

In recent years, DFT method are widely used for structural characteristics of BPs and HAP and interaction between them^{3,38,47}. The surface energetics of HAP crystalline surfaces using ab initio density functional theory (DFT) calculations within the generalized gradient approximation (GGA) for the exchange-correlation functional has been studied by

Zhu and Wu⁴⁷, testing the effects of slab thickness, vacuum width between slabs, and surface relaxation on surface energy. Barrios³ has investigated the interaction between collagen protein and HAP surface by using a combination of computational techniques, DFT and classical MD methods. More recently, the adsorption process of zoledronate on HAP (001) surface were examined in detail, which showed that the significant charge movement between BPs and HAP (001) surface occurs and the strong binding affinity of zoledronate with HAP is due to structural similarity³⁸.

In this paper, using ab initio DFT method, the molecular structures of 8 BPs (clodronate, etidronate, pamidronate, alendronate, ibandronate, risedronate, zoledronate, and minodronate) are obtained, and the binding affinity is evaluated via their adsorption energies onto HAP (001) surface.

2 Computational Method

DFT calculations are performed together with molecular mechanics (MM) calculations. MM is less expensive computationally, but not more accurate and precise than DFT. Therefore, MM is needed to find rough and globally-optimised structures using simulated annealing³⁹, in which the temperature is increased from 300K to 5000K, and decreased back to 300K in 100,000 steps. For MM calculations, we have used GULP (General Utility Lattice Program) code²⁵ with Dreiding forcefield⁴³ and QEq atomic charges². Globally-optimised rough structure obtained in MM calculation goes for more accurate and precise structural relaxation in DFT calculation.

For DFT calculations, we have employed SIESTA code⁴⁴ which solves numerically Kohn-Sham equation within DFT^{22,29} using a localized numerical basis set, namely pseudo atomic orbitals, and pseudopotentials for describing the interaction between ionic core (nucleus plus core electrons) and valence electrons. The BLYP GGA functional (the Becke exchange functional¹ in conjunction with the Lee-Yang-Parr correlation functional⁵) is used for exchange-correlation interaction between electrons. For all the atoms, Troullier-Martins³² type norm-conserving pseudopotentials are generated within local density approximation (LDA)²⁶, and the DZP type (double f plus polarization) basis sets are used. The mesh size of grid, which is controlled by energy cutoff to set the wavelength of the shortest plane wave represented on the grid, has taken a value of 200 Ry. Non-fixed atoms are allowed to relax until the forces converge less than 0.02 eV/Å².

To simulate adsorption of BPs onto HAP surface, initial configuration of BPs adsorbed onto HAP surface must be given, from which globally-optimized configuration is obtained using simulated annealing in MM and further relaxation in DFT.

The adsorption energy of BPs onto HAP surface is given by

$$E_{\text{ads}} = E_{\text{system}} - (E_{\text{HAP}} + E_{\text{BP}}), \quad (1)$$

where E_{HAP} is the energy of surface slab, E_{BP} , the energy of isolated BP molecule, and E_{system} , the total energy of system consisted of HAP surface slab and BP molecule adsorbed on it.

3 Results and Discussion

Table 2 provides structural parameters of globally-optimized BPs structures, in which O(H) means oxygen atom linked to hydrogen atom, and P=O means double bond between phosphorous atom and oxygen atom. Bond length of C–R2 depends on R1 largely and bond length of P–C and bond angle of P–C–P vary significantly with R2, while other parameters remain almost unchanged, from which P–C–P structure is shown to be mainly related with binding affinity. Also, π -bond of P=O reduces bond length compared to P–O(H).

Structural and lattice parameters of HAP crystal and surface are provided in Table 3, where HAP crystal is doubled along one axis normal to the orientation of hydroxyl group to keep its practical isotropy (See Figure 3). For convenience, Ca atoms on Layer 1 are presented by Ca1, and those on Layer 2 by Ca2. Comparison of structural parameters of BPs with

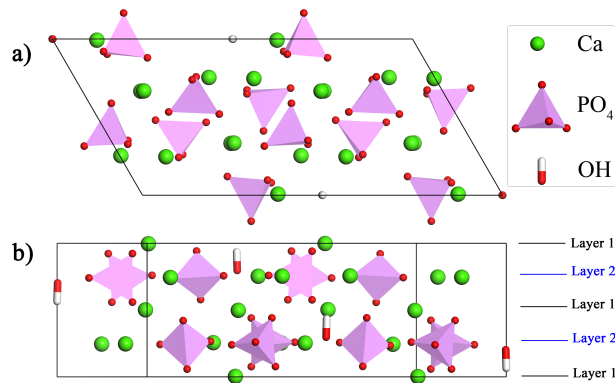


Fig. 3 Crystal Structure of Hydroxyapatite, a) Top View, b) Side View.

those of HAP (Table 3) shows that P–O(H) bond lengths of BPs (1.62~1.64) are similar to those of HAP (1.578 for crystal, 1.583 for surface).

Figure 4 presents HOMO and LUMO of BPs which shows that HOMO is distributed around nitrogen atom for N-BPs and nitrogen atom behaves as electron donor in adsorption process.

Table 4 provides Hirshfeld charges²¹ of BPs, in which O(=P) means oxygen atom double-bonding to phosphorous atom, and O(H) means oxygen atom linked to hydrogen atom. As

Table 3 Lattice Parameters of HAP crystal and surface

Lattice Parameters		
a, b, c	18.695, 9.354, 6.956	
α, β, γ	90, 90, 119.86	
Structural Parameters		
	Crystal	Surface
Average of bond lengths		
P–O	1.578	1.583
Ca1–O	2.423	2.352
Ca2–O	2.553	2.434
Average of bond angles		
O–P–O	109.44	109.39
O–Ca1–O	98.62	101.50
O–Ca2–O	99.40	94.01

shown in Table 4, Hirshfeld charges of phosphorous atom and oxygen atoms double-bonding to former remain almost unchanged, and those of R1, R2, and carbon atom between two phosphorous atoms change significantly.

Figure 5 shows the adsorption geometries of BPs onto HAP (001) surface, which indicates that hydrogen bond between OH of BPs and O of HAP plays an important role in strong binding of BPs onto hydroxyapatite.

Table 5 shows Hirshfeld charges of HAP crystal and surface (before and after BPs adsorption). As shown in Table 5, atomic charges of surface differ remarkably from those of crystal before adsorption, while the adsorption of BPs relaxes atomic charges of HAP surface towards those of crystal, so that the adsorption of BPs stabilizes HAP surface.

Table 6 shows the adsorption energies of BPs onto HAP(001) surface, which indicates that PAM has the greatest value, followed by ALN, ZOL, CLO, IBN, RIS, MIN, and ETD, which parallels the ranking orders of Table 1.

Table 6 Adsorption Energies of BPs onto HAP(001) surface.

	E_{BP} (eV)	E_{HAP} (eV)	$E_{\text{BP-HAP}}$ (eV)	E_{Ads} (eV)
CLO	-3997.45	-50669.94	-54669.74	-2.35
ETD	-3840.24	-50669.94	-54512.35	-2.17
PAM	-4313.33	-50669.94	-54986.60	-3.33
ALN	-4500.17	-50669.94	-55173.33	-3.21
IBN	-5436.13	-50669.94	-56108.38	-2.31
RIS	-4931.92	-50669.94	-55604.11	-2.25
ZOL	-4876.41	-50669.94	-55549.28	-2.92
MIN	-5528.59	-50669.94	-56200.71	-2.17

4 Conclusions

In this paper, the geometries of BPs were studied to find out that P–C–P structure is sensitive to R2 group and mainly cor-

Table 2 Structural Parameters of BPs. P–O(H) means single bond between phorous atom and oxygen atom linked to hydrogen atom, and P=O means double bond between phorous atom and oxygen atom.

	CLO	ETD	PAM	ALN	IBN	RIS	ZOL	MIN
Bond Length								
P–O(H)	1.62	1.64	1.64	1.64	1.63	1.64	1.63	1.63
P=O	1.49	1.49	1.49	1.48	1.49	1.48	1.49	1.49
P–C	1.88	1.99	1.94	1.93	1.90	1.95	1.97	1.90
C–R1	1.78	1.40	1.40	1.41	1.41	1.39	1.40	1.41
C–R2	1.78	1.55	1.56	1.56	1.54	1.58	1.57	1.58
Bond Angle								
(H)O–P–O(H)	97.0	96.9	96.4	95.4	99.2	95.1	97.3	102.1
O=P–O(H)	119.5	116.8	116.9	118.2	116.5	118.8	116.5	116.1
C–P–O(H)	105.1	110.4	109.6	106.9	106.1	107.0	110.3	105.2
C–P=O	108.9	105.8	107.0	109.9	111.3	108.5	105.7	111.0
P–C–P	102.4	93.7	94.3	98.6	96.9	101.1	90.9	94.6
P–C–R1	110.2	110.9	113.2	107.7	109.0	113.2	112.9	109.1
P–C–R2	110.1	113.8	112.8	115.7	113.0	108.6	114.9	114.7
R1–C–R2	113.4	112.8	110.2	110.6	114.6	111.4	109.9	112.8

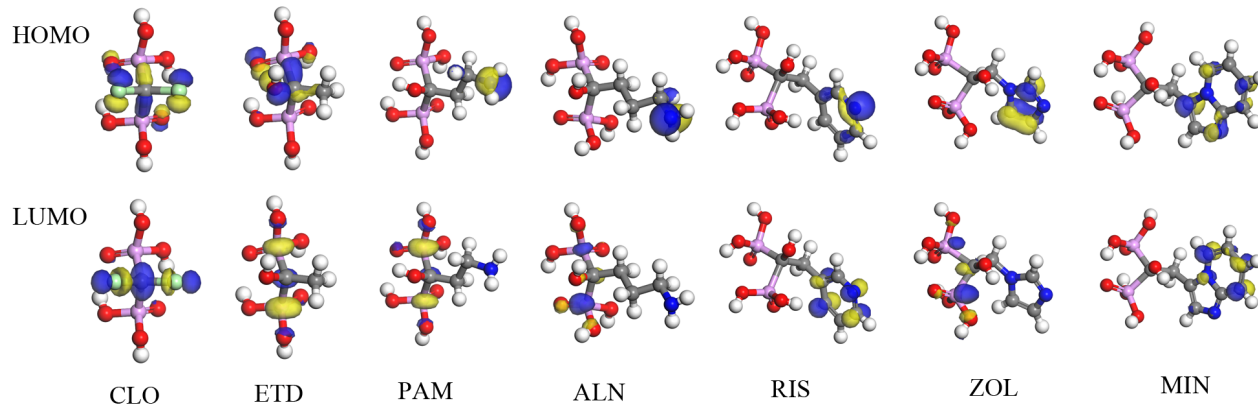


Fig. 4 HOMO and LUMO of BPs

Table 4 Hirshfeld Charges of BPs. O(=P) means oxygen atom double-bonding to phorous atom, and O(H) means oxygen atom linked to hydrogen atom.

	CLO	ETD	PAM	ALN	IBN	RIS	ZOL	MIN
C	-0.025	0.045	0.038	0.025	0.014	0.034	0.032	0.007
P	0.490	0.498	0.494	0.494	0.500	0.496	0.500	0.501
O(=P)	-0.336	-0.353	-0.355	-0.358	-0.334	-0.343	-0.342	-0.335
H	0.152	0.157	0.154	0.162	0.142	0.160	0.153	0.147
O(H)	-0.221	-0.234	-0.227	-0.229	-0.222	-0.234	-0.224	-0.221
R1	0.002	-0.055	-0.041	-0.056	-0.043	-0.043	-0.053	-0.068
R2	0.003	0.027	0.021	0.026	0.022	-0.003	-0.013	0.029

related to binding affinity onto hydroxyapatite crystal. For N-BPs, nitrogen atom is shown to behaves as donor during the adsorption through HOMO and LUMO analysis.

process, charges of BPs and HAP change reamarkably, and BPs adsorption relaxes charges of HAP surface towards those of HAP crystal, so that it can stabilize HAP surface.

Hirshfeld charge analysis shows that during the adsorption

The adsorption geometries of BPs onto hydroxyapatite

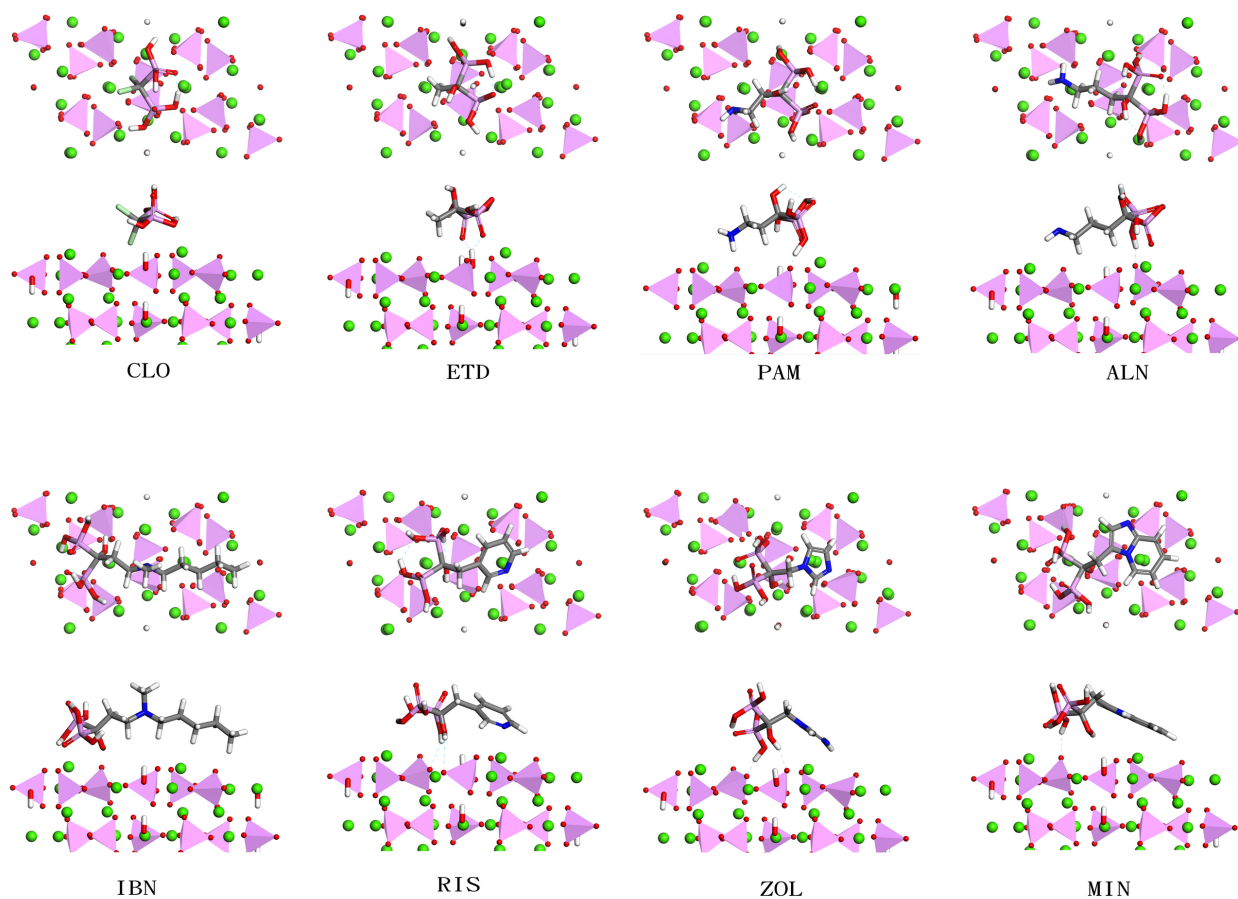


Fig. 5 Adsorption Geometries of BPs onto HAP (001) surface.

Table 5 Hirshfeld Charges of HAP crystal and surface. Ca1 means calcium atom on Layer 1, Ca2 means calcium atom on Layer 2, O1, O2 and O3 mean oxygen atoms of phosphate tetrahedron, in which O1 places on Layer 1, and O2 and O3 on Layer 2.

Element	Crystal	Surface	HAP Surface combined with BPs							
			CLO	ETD	PAM	ALN	IBN	RIS	ZOL	MIN
Ca1	0.429	0.783	0.555	0.616	0.592	0.553	0.550	0.516	0.532	0.524
Ca2	0.415	0.508	0.460	0.478	0.479	0.471	0.471	0.468	0.477	0.478
O1	-0.290	-0.377	-0.358	-0.347	-0.335	-0.340	-0.348	-0.349	-0.341	-0.351
O2	-0.283	-0.318	-0.314	-0.308	-0.310	-0.310	-0.310	-0.313	-0.304	-0.312
O3	-0.296	-0.312	-0.309	-0.290	-0.307	-0.308	-0.307	-0.307	-0.307	-0.309
P	0.533	0.481	0.494	0.501	0.502	0.502	0.498	0.499	0.503	0.497
H	0.130	0.128	0.120	0.130	0.130	0.130	0.130	0.131	0.136	0.135
O(H)	-0.355	-0.356	-0.359	-0.366	-0.362	-0.359	-0.356	-0.358	-0.362	-0.358

(001) surface shows that hydrogen bond between OH of BPs and O of HAP plays an important role in strong binding of BPs onto hydroxyapatite.

Comparing the adsorption energies of BPs onto hydroxyapatite (001) surface, obtained by first-principles calculation, pamidronate has the greatest value, and etidronate has the low-

est value, which parallels the experimental ranking order, i.e. adsorption energy is the main factor determining the binding affinity of BPs onto hydroxyapatite.

References

- 1 Becke AD. Density-functional exchange-energy approximation with correct asymptotic behavior. *Phys Rev A*, 38:3098-100, 1988.
- 2 Rappe AK and Goddard WA. *J. Phys. Chem.*, 95:3358, 1991.
- 3 N. A. Barrios. *A Computational Investigation of the Interaction of the Collagen Molecule with Hydroxyapatite*. PhD thesis, Department of Chemistry, University College London, 2010.
- 4 Benedict. The physical chemistry of the diphosphonates-its relationship to their medical activity. In Donath A and Courvoisier B, editors, *Symposium CEMO IV. Diphosphonates and bone*, pages 1–19. 1995.
- 5 Lee C, Yang W, and Parr RG. Development of the Colle-Salvetti correlation-energy formula into a functional of the electron density. *Phys Rev B*, 37:7859, 1988.
- 6 Leu CT, Luegmayr E, Freedman LP, Rodan GA, and Reszka AA. Relative binding affinities of bisphosphonates for human bone and relationship to antiresorptive efficacy. *Bone*, 38:628–36, 2006.
- 7 Black DM, Delmas PD, Eastell R, Reid IR, Boonen S, and et al. Cauley JA. Once-yearly zoledronic acid for treatment of postmenopausal osteoporosis. *N Engl J Med*, 356:809–22, 2007.
- 8 L. F. Duarte, F. C. Teixeira, and R. Fausto. Molecular modeling of the interaction of novel hydroxyl- and aminobisphosphonates with hydroxyapatite. *ARKIVOC*, (v):117, 2010.
- 9 Oldfield E. Targeting isoprenoid biosynthesis for drug discovery: bench to bedside. *Acc Chem Res*, 43:1216–26, 2010.
- 10 Van Beek E, Lwjk C, and Que I et al. Dissociation of binding and antiresorptive properties of hydroxybisphosphonates by substitution of the hydroxyl with an amino group. *J Bone Miner Res*, 11(10):1492-97, 1996.
- 11 Ebetino FH, Hogan A-ML, Sun S, Tsoumpra MK, Duan X, Trifft JT, Kwaasi AA, Dunford JE, Barnett BL, Oppermann U, Lundy MW, Boyde A, Kashemirov BA, McKenna CE, and Russell RGG. The relationship between the chemistry and biological activity of the bisphosphonates. *Bone*, 49:20–33, 2011.
- 12 Ebetino FH, Barnett BL, and Russell RGG. A computational model delineates differences in hydroxyapatite binding affinities of bisphosphonate [abstract]. *J Bone Miner Res*, 20(Suppl 1):S259, 2005.
- 13 Ebetino FH and Dansereau. Bisphosphonates antiresorptive structure-activity relationship. In Bijvoet OLM, Fleisch HA, Canfield RE, and Russell RGG, editors, *Bisphosphonate on bones*, pages 139–53. Elsevier, 1995.
- 14 Ebetino FH, Francis MD, and Rogers MJ et al. Mechanisms of action of etidronate and other bisphosphonates. *Rev Contemp Pharmacother*, 9:23343, 1998.
- 15 Coxon FP, Thompson K, and Rogers MJ. Recent advances in understanding the mechanism of action of bisphosphonates. *Curr Opin Pharmacol*, 6:307312, 2006.
- 16 Kontecka E. G, Jezierska J, Lecouvey M, Leroux Y, and Kozlowski H. *J. Inorg. Biochem*, 89:13, 2002.
- 17 Owens G, Jackson R, and An integrated approach: bisphosphonate management for the treatment of osteoporosis Lewiecki EM. *Am J Manag Care*, 13(Suppl 1):S290–308, 2007.
- 18 Nancollas GH, Tang R, Phipps RJ, Henneman Z, Gulde S, and et al. Wu W. Novel insights into actions of bisphosphonates on bone: differences in interactions with hydroxyapatite. *Bone*, 38:617–27, 2006.
- 19 Fleich H. *Endocr. Rev*, 19:80, 1998.
- 20 Fleisch HA, Russell RG, Bisaz S, Muhlbauer RC, The inhibitory effect of phosphonates on the formation of calcium phosphate crystals in vitro Williams DA, on aortic, and kidney calcification in vivo. *Eur J Clin Invest*, 1:12–18, 1970.
- 21 F. L. Hirshfeld. Bonded-atom fragments for describing molecular charge densities. *Theor. Chim. Acta B*, 44:129, 1977.
- 22 P. Hohenberg and W. Kohn. Inhomogeneous electron gas. *Phys. Rev.*, 136:B864–71, 1964.
- 23 Roelofs A. J, Thompson K, Gordon S, and Rogers M. J. *Clin. Cancer Res*, 12:6222, 2006.
- 24 Rogers M. J, Gordon S, Benford H. L, Coxon F. P, Luckman S. P, Monkkonen J, and J. C Frith. *Cancer Suppl*, 8:2961, 2000.
- 25 Gale JD and Rohl AL. The general utility lattice program (gulp). *Mol Simul*, 29:291341, 2003.
- 26 Perdew JP and Zunger A. Self-interaction correction to density-functional approximations for many-electron systems. *Phys Rev B*, 23:5048, 1981.
- 27 Green JR, Mueller K, and Jaeggi KA. Preclinical pharmacology of cgp 42 446, a new, potent, heterocyclic bisphosphonate compound. *J Bone Miner Res*, 9:745 51, 1994.
- 28 Goa KL and Balfour JA. Risedronate. *Drugs Aging*, 13:83 91, 1998.
- 29 W. Kohn and L. J. Sham. Self-consistent equations including exchange and correlation effects. *Phys. Rev.*, 140:A1133–8, 1965.
- 30 M. A. Lawson, Z. Xia, B. L. Barnett, J. T. Trifft, R. J. Phipps, J. E. Dunford, R. M. Locklin, F. H. Ebetino, and R. G. G. Russell. Differences between bisphosphonates in binding affinities for hydroxyapatite. *J Biomed Mater Res B Appl Biomater*, 92:149–55, 2010.
- 31 Lawson MA, Trifft JT, and Ebetino FH et al. Potential bone mineral binding differences among bisphosphonates can be demonstrated by the use of hydroxyapatite column chromatography [abstract]. *J Bone Miner Res*, 20(Suppl 1):S396, 2005.
- 32 Troullier N and Martins JL. Efficient pseudopotentials for plane-wave calculations. *Phys Rev B*, 43:19932006, 1991.
- 33 Bartl R, Frisch B, von Tresckow E, and Bartl C. *Bisphosphonates in Medical Practice*. Springer-Verlag, Berlin, 2007.
- 34 Russell RG, Muhlbauer RC, Bisaz S, Williams DA, and Fleisch H. The influence of pyrophosphate, condensed phosphates, phosphonates and other phosphate compounds on the dissolution of hydroxyapatite in vitro and on bone resorption induced by parathyroid hormone in tissue culture and in thyroparathyroidectomised rats. *Calcif Tissue Res*, 6:183–96, 1970.
- 35 Russell RG, Xia Z, Dunford JE, Oppermann U, Kwaasi A, and et al. Hullely PA. Bisphosphonates: an update on mechanisms of action and how these relate to clinical efficacy. *Ann N Y Acad Sci*, 1117:209–57, 2007.
- 36 Russell RGG. Bisphosphonates: the first 40 years. *Bone*, 49:219, 2011.
- 37 Russell RGG, Watts NB, Ebetino FH, and Rogers MJ. Mechanisms of action of bisphosphonates: similarities and differences and their potential influence on clinical efficacy. *Osteoporos Int*, 19:733759, 2008.
- 38 MH Ri, CJ Yu, YM Jang, and SU Kim. Ab initio investigation of the adsorption of zoledronic acid molecule on hydroxyapatite (001) surface: an atomistic insight of bone protection. *J Mat Sci*, 51:3125–35, 2016.
- 39 Kirkpatrick S, Gelatt CD, and Vecchi MP. Optimization by simulated annealing. *Science*, 220:671–80, 1983.
- 40 Mukherjee S, Huang C, Guerra F, Wang K, and Oldfield E. Thermodynamics of bisphosphonates binding to human bone: a two-site model. *J Am Chem Soc*, 131:8374–5, 2008.
- 41 Mukherjee S, Song Y, and Oldfield E. Nmr investigations of the static and dynamic structures of bisphosphonates on human bone: a molecular model. *J Am Chem Soc*, 130:1264–73, 2008.
- 42 Papapoulos SE, Hoekman K, Lowik CWGM, Vermeij P, and Bijvoet OLM. Application of an in vitro model and a clinical protocol in the assessment of the potency of a new bisphosphonate. *J Bone Miner Res*, 4:775 81, 1988.
- 43 Mayo SL, Olafson BD, and Goddard WA. Dreiding: A generic forcefield. *J. Phys. Chem.*, 94:8897–909, 1990.
- 44 J. M. Soler, E. Artacho, J. D. Gale, A. García, J. Junquera, P. Ordejón, and D. Sánchez-Portal. The siesta method for ab initio order-n materials simulation. *J. Phys:Condens. Matter*, 14:2745, 2002.
- 45 Luckman SP, Coxon FP, and Ebetino FH et al. Heterocycle-containing bisphosphonates cause apoptosis and inhibit bone resorption by preventing protein prenylation: evidence from structure-activity relationships in j774 macrophages. *J Bone Miner Res*, 13(11):1668–78, 1998.
- 46 Jahnke W and Henry C. An in vitro assay to measure targeted drug deliv-

-
- ery to bone mineral. *Chem Med Chem*, 5:770–6, 2010.
- 47 Zhu W and Wu P. Surface energetics of hydroxyapatite: a dft study. *Chem Phys Lett*, 396:3842, 2004.
- 48 Volkert WA and Hoffman TJ. *Chem. Rev.*, 99:2269, 1999.
- 49 Duan X, Xia Z, Zhang H, Quijano M, Dobson RLM, and et al. Triffit JT. The effects of ph on the relative bone mineral-binding affinities of bisphosphonates determined by hydroxyapatite-column chromatography. *J Bone Miner Res*, 25(Suppl 1):S347, 2010.